

# Towards a Composite Framework for Simultaneous Exploration of New Physics in Background and Perturbed Universes

Shibendu Gupta Choudhury,<sup>1,\*</sup> Purba Mukherjee,<sup>1,†</sup> and Anjan Ananda Sen<sup>1,‡</sup>

<sup>1</sup>*Centre for Theoretical Physics, Jamia Millia Islamia, New Delhi-110025, India*

We investigate deviations from  $\Lambda$ CDM by independently parameterizing modifications in the background evolution and the growth of structures. The background is characterized by two parameters,  $A$  and  $B$ , which reduce to  $\Omega_{m0}$  and  $2/3$  in the  $\Lambda$ CDM limit, while deviations in the growth of structures are captured through a new fitting function for  $f\sigma_8$  involving the growth index  $\gamma$ . Using recent observational datasets, we find significant evidence for departures from  $\Lambda$ CDM, with data suggesting a preference for modifications in the background evolution, likely due to evolving dark energy, rather than modifications to gravity. Additionally, our framework alleviates the  $H_0$  tension and addresses the  $\sigma_8$  and  $S_8$  tensions. We also demonstrate that future high-precision RSD data could unveil correlations between background and perturbation parameters that are currently suppressed by observational uncertainties, offering deeper insights into cosmic evolution.

Keywords: cosmology, reconstruction, cosmological parameters, dark energy

## I. INTRODUCTION

The  $\Lambda$ CDM model, which assumes General Relativity (GR) as the underlying theory of gravity and a spatially flat universe having approximately 70% Dark Energy (DE) (with constant energy density described by a cosmological constant  $\Lambda$ ) and 30% Cold Dark Matter (CDM), provides an excellent agreement with observations [1]. This includes fluctuations in the temperature and polarization of the cosmic microwave background (CMB) [2–4], observations involving the large-scale structure (LSS) of the universe [5–8], the distance-redshift relation of Type Ia supernovae (SNIa) [9, 10], etc. However, recent observations suggest a significant deviation from this concordance model. For example, when baryon acoustic oscillation (BAO) measurements from the Dark Energy Spectroscopic Instrument (DESI) [11] are combined with SNIa [12–14] and CMB [2, 4] observations, it indicates  $\approx 3 - 4\sigma$  deviation from  $\Lambda$ CDM. More importantly, there is a  $> 5\sigma$  tension between the present values of Hubble parameter  $H_0$  from direct measurements [15] vs that inferred from the early CMB sky [2]. Though less significant than  $H_0$  tension, the parameter  $S_8 \equiv \sigma_{8,0} \sqrt{\Omega_{m0}}/0.3$  ( $\sigma_{8,0}$  being the variance of matter density fluctuations in a sphere of comoving radius  $8 h^{-1}$  Mpc and  $\Omega_{m0}$  being the matter density relative to the critical density at present epoch) obtained from CMB observations is found to be larger than  $S_8$  determined from observations of galaxy clustering and weak lensing [16]. Furthermore, several theoretical challenges persist, such as the elusive nature of dark matter, the cosmological constant problem, and the coincidence problem [17]. These unresolved issues provide strong motivation to explore potential deviations from  $\Lambda$ CDM and investigate alternative cosmological frameworks [18, 19].

Several approaches have been proposed so far to model deviations from  $\Lambda$ CDM. They can be broadly classified into two scenarios: (i) modification in the DE sector or (ii) modification in the gravity sector. In the first class,  $\Lambda$  is replaced by a component for which the equation of state (EoS) for DE  $w_{\text{DE}}$  is either constant (but  $\neq -1$ ) or has a scale-factor dependence [20, 21]. The latter represents a large family of dynamical dark energy models (DDE) [21–23] and GR is assumed to be the governing theory in these models. The other class represents models where pressure-less matter is the only energy component of the Universe and late-time acceleration of the Universe occurs due to modification of gravity at cosmological scales. This includes modified gravity (MG) theories like  $f(R)$  gravity [24, 25], scalar-tensor theories [26], Cardassian models [27] and other alternatives [28, 29].

In recent years, reconstruction methods have become increasingly popular in cosmology [30]. These include non-parametric techniques to infer the underlying cosmic evolution directly from data [31–34] or parametrization(s) that can introduce flexible yet physically motivated modifications to key cosmological functions [20, 35–38]. In this work, we adopt the latter for examining deviations from  $\Lambda$ CDM in both the background evolution and the growth of cosmic structures. Rather than adopting a single unified modification (as studied in [39, 40]), we attempt to model deviations separately in the background and perturbation sectors. This framework allows us to explore potential new physics in each sector independently. To capture deviations in the background sector, we adopt the formalism discussed in [37, 41], where modifications are introduced in the late-time evolution of the scale factor, the most fundamental quantity governing cosmological evolution. This general formalism is quite robust to account for both DE and MG scenarios (see [41] for details). Following [39, 40], which emphasize the importance of isolating and constraining the growth of structures separately from geometrical quantities to better understand the underlying cosmology, we construct a new fitting function for growth rate  $f\sigma_8$ , where  $f$  is

\* pdf.schoudhury@jmi.ac.in

† pdf.p Mukherjee@jmi.ac.in

‡ aasen@jmi.ac.in

the logarithmic growth factor. This fitting function can systematically characterize the growth of perturbations and identify possible deviations from  $\Lambda$ CDM in the perturbed universe. We constrain the background evolution and growth of perturbations by considering low redshift SNIa and BAO data, along with growth rate measurements from redshift space distortions (RSD).

This paper is organized as follows: We discuss the underlying theoretical framework in section II. We briefly mention the datasets and methodology used to conduct our analysis in section III and explicitly discuss the results in section IV. In section V, we demonstrate how more precise RSD data, expected from future surveys, can significantly enhance our understanding of cosmic evolution. The final section VI presents some concluding remarks.

## II. THEORETICAL FRAMEWORK

We know that for the  $\Lambda$ CDM model, the late time behaviour of the scale factor of the Universe is given by,

$$a(t) = a_1 [\sinh(t/\tau)]^{\frac{2}{3}}. \quad (1)$$

Here  $a_1$  is an arbitrary dimensionless parameter, and  $\tau$  is an arbitrary parameter of dimension  $[T]$ . The resulting Hubble parameter  $H(z)$  is,

$$H(z) = H_0 [\Omega_{m0}(1+z)^3 + (1 - \Omega_{m0})]^{\frac{1}{2}}, \quad (2)$$

where  $H_0$  is the current value of the Hubble parameter and  $\Omega_{m0}$  is the current fractional matter density parameter given by,  $\Omega_{m0} = \frac{\rho_{m0}}{3H_0^2/8\pi G}$ . We define the reduced Hubble factor as,

$$E(z) \equiv H(z)/H_0 = \sqrt{\Omega_{m0}(1+z)^3 + (1 - \Omega_{m0})}. \quad (3)$$

The fractional matter density parameter  $\Omega_m$  at some redshift  $z$  is given by,

$$\Omega_m(z) = \frac{\Omega_{m0}(1+z)^3}{E^2(z)}. \quad (4)$$

Next, we consider a recently proposed minimal extension of  $a(t)$  to represent any new physics dominating the background evolution, irrespective of any specific DE model or MG theory [41],

$$a(t) = \tilde{a}_1 [\sinh(t/\tau)]^B, \quad (5)$$

where  $\tilde{a}_1$  and  $B$  are dimensionless arbitrary parameters. Accordingly, the expression for  $E(z)$  comes out to be,

$$E(z) = \left[ A(1+z)^{2/B} + (1 - A) \right]^{\frac{1}{2}}. \quad (6)$$

Here,  $H_0 = \frac{B}{\tau\sqrt{1-A}}$  is the Hubble parameter at present epoch, and  $A = \frac{\tilde{a}_1^{2/B}}{1+\tilde{a}_1^{2/B}}$ . We can retrieve the  $H(z)$  for

$\Lambda$ CDM with the identification  $A = \Omega_{m0}$  and  $B = 2/3$  in Eq. (6). This modified evolution can have several origins that are explicitly discussed in [41]. However, in this work, we do not focus on these origins. Instead, we assume that the parameters  $A$  and  $B$  characterize a generic framework for modified background evolution and encode any potential new physics in the background sector.

Similarly, any new physics in the perturbation sector can be treated distinctly, as we describe next. At late times, the evolution of matter density contrast  $\delta = \delta\rho_m/\rho_m$  within the framework of  $\Lambda$ CDM is governed by the following equation,

$$\delta'' + \frac{1}{a} \left( 3 + \frac{a E'}{E} \right) \delta' - \frac{3\Omega_{m0}}{2a^5 E^2} \delta = 0, \quad (7)$$

where  $\prime$  denotes differentiation with respect to  $a$ . Note that the presence of  $\Omega_{m0}$  (the matter contribution in the Universe) in the above equation originates from Poisson's equation, where we assume that only matter clusters at relevant scales. This is important because even if the DE sector contains a term which scales as  $\sim (1+z)^3$ , that will not contribute to Poisson's equation. On the other hand, the term  $\frac{E'}{E}$  in the above equation contains contributions from both matter and DE through Eq. (6).

A robust parametrization for the logarithmic growth factor  $f \equiv \frac{d \ln \delta}{d \ln a}$  is given by [22, 42, 43],

$$f = \Omega_m^\gamma, \quad (8)$$

where  $\gamma$  is the growth index parameter. With GR as the underlying theory, flat  $\Lambda$ CDM background predicts  $\gamma = 6/11$ , and this fit is accurate to 0.1% [22, 44, 45]. Note that in the concordance  $\Lambda$ CDM model, the linear matter density fluctuation  $\delta$  is governed solely by the background evolution. Therefore, any deviation from  $\gamma = 6/11$  would indicate a potential new physics affecting the growth of structure beyond what is dictated by background evolution alone.

As our first step, we construct a suitable fitting form for  $f\sigma_8$  as a function of  $\Omega_m$  to introduce new physics in the perturbation sector. The primary motivation comes from the fact that observational data usually involve  $f\sigma_8$  rather than  $f$  alone. A well-constructed fitting form will thus offer a more convenient way to introduce modifications in the perturbation sector while keeping the background sector unaffected.

The evolution of  $\sigma_8$  is defined as  $\sigma_8 = \sigma_{8,0} \frac{\delta(a)}{\delta(1)}$ , where  $\sigma_{8,0}$  is its present value. To express  $\sigma_8$  as a function of  $\Omega_m$  we note,

$$\frac{d \log \delta}{d \Omega_m} = \frac{\Omega_m^{\gamma-1}}{3(\Omega_m - 1)}, \quad (9)$$

as derived from Eqs. (3), (4), and (8). Thus, we arrive at the solution for  $\delta$ , as

$$\delta(\Omega_m) = A \exp \left[ -\frac{\Omega_m^\gamma {}_2F_1(1, \gamma; \gamma + 1; \Omega_m)}{3\gamma} \right], \quad (10)$$

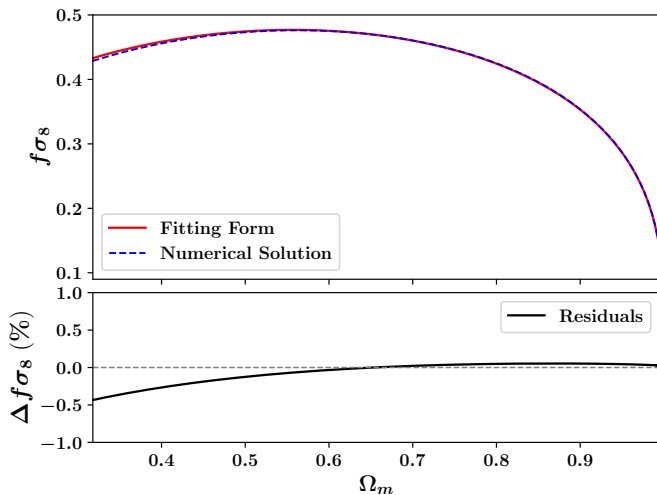


FIG. 1. Plots for  $f\sigma_8$  values as a function of  $\Omega_m$  obtained using the fitting form in Eq. (11) (red line) and from solving Eq. (7) (dashed blue line). Here we have used  $\Omega_{m0} = 0.315$ ,  $\sigma_{8,0} = 0.811$ ,  $\gamma = \frac{6}{11}$  and assumed  $\delta(a) \approx a$  and  $\delta'(a) \approx 1$  in the matter dominated era.

where  ${}_2F_1(a, b; c; x)$  is the Gauss Hypergeometric function. Therefore,

$$f\sigma_8(\Omega_m) = \sigma_{8,0} \Omega_m^\gamma \exp \left[ \frac{\Omega_{m0}^\gamma}{3\gamma} {}_2F_1(1, \gamma; \gamma + 1; \Omega_{m0}) - \frac{\Omega_m^\gamma}{3\gamma} {}_2F_1(1, \gamma; \gamma + 1; \Omega_m) \right]. \quad (11)$$

The above expression provides a new fitting form for  $f\sigma_8$  as a function of  $\Omega_m$ . This function closely matches with the  $f\sigma_8$  values obtained by solving Eq. (7) for the  $\Lambda$ CDM model with  $\gamma = 6/11$ . Fig. 1 illustrates this agreement by comparing the fitting function in (11) with the numerical solution of the growth equation (Eq. (7)), showing  $f\sigma_8$  as a function of  $\Omega_m$ . As evident from Fig. 1, this fitting function describes the  $f\sigma_8$  behaviour for  $\Lambda$ CDM model very accurately. By modelling  $f\sigma_8$  using Eq. (11), any new physics in the perturbation sector will be captured by the parameter  $\gamma$ .

In what follows, we utilize Eq. (6) and Eq. (11) to represent the background evolution and growth of perturbations, respectively. This defines our composite model with parameters  $A$ ,  $B$ ,  $\Omega_{m0}$ ,  $\gamma$  and  $\sigma_{8,0}$ , which we constrain employing different observational datasets and their combinations. In the  $\Lambda$ CDM model,  $B = 2/3$ ,  $\gamma = 6/11$  and  $A \equiv \Omega_{m0}$ . Deviations from any of these conditions would indicate potential new physics in either background or in perturbed Universe or in both.

### III. DATA AND METHODOLOGY

We make use of the following datasets in our analysis:

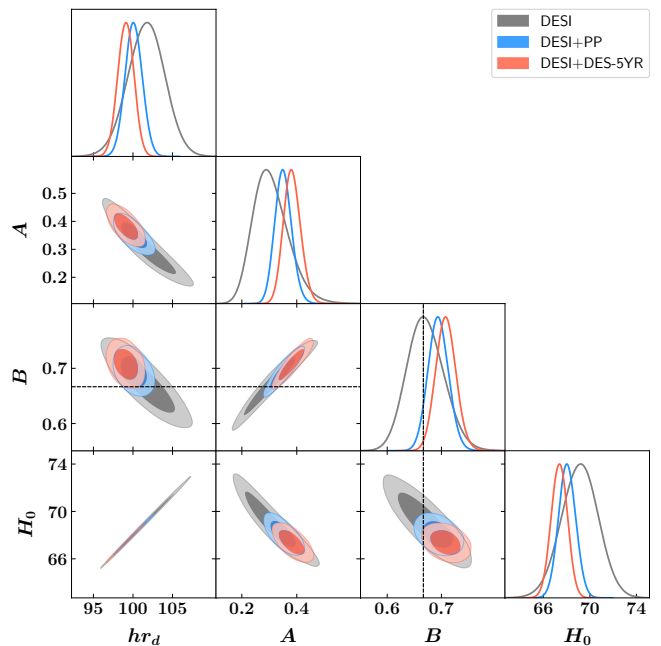


FIG. 2. One-dimensional marginalized posterior distributions, 2-dimensional contour plots at 68% and 95% C.L. limits for relevant parameters of the composite model using BAO and SNIa datasets.

- **BAO:** We utilize 12 correlated BAO distance measurements from DESI-DR1 spanning the redshift range  $0.1 < z < 4.2$ , assembled in Table 1 of [11]. For convenience, we refer to this dataset as ‘DESI’ hereafter.
- **SNIa:** We consider two SNIa datasets, namely the Pantheon-Plus [14] compilation and sample provided by 5 years of the Dark Energy Survey (DES) Supernova program [46]. We refer to them as ‘PP’ and ‘DES-5YR’, respectively.
- **RSD:** We consider the  $f\sigma_8$  data compiled by Nesseris *et al.* [47], Sagredo *et al.* [48] and Skara and Perivolaropoulos [49] and include the covariance matrices of the data from the WiggleZ [50] and SDSS-IV [51] compilation. We also incorporate the correction from the Alcock-Paczynski (AP) effect by considering the corresponding fiducial cosmology [52]. We refer to this dataset as ‘RSD’.

Here we have two parameters in the background sector, namely,  $A$  and  $B$ , along with  $hr_d$ , where  $h = \frac{H_0}{100 \text{ km s}^{-1} \text{ Mpc}^{-1}}$  is the dimensionless Hubble constant and  $r_d$  is the sound horizon at the drag epoch. In the perturbation sector, we have three more parameters:  $\Omega_{m0}$ ,  $\gamma$  and  $\sigma_{8,0}$ , in addition to  $A$  and  $B$ . Assuming uniform priors on all parameters, we undertake a Bayesian Markov Chain Monte Carlo (MCMC) analysis to constrain the composite model, utilizing the `emcee`<sup>1</sup> package. The

<sup>1</sup> Available at: <http://dfm.io/emcee/current/>

Datasets	$hr_d$	$A$	$B$	$\Omega_{m0}$	$\gamma$	$\sigma_{8,0}$	$H_0$	$S_8$
RSD	-	$0.43^{+0.19}_{-0.23}$	$0.605^{+0.078}_{-0.10}$	$0.33 \pm 0.16$	$0.95^{+0.30}_{-0.61}$	$1.01^{+0.11}_{-0.26}$	-	$1.02 \pm 0.32$
DESI	$101.7 \pm 2.3$	$0.305^{+0.052}_{-0.073}$	$0.671^{+0.031}_{-0.036}$	-	-	-	$69.13 \pm 1.68$	-
DESI+PP	$100.1 \pm 1.1$	$0.351^{+0.028}_{-0.032}$	$0.694 \pm 0.019$	-	-	-	$68.06 \pm 0.87$	-
DESI+DES-5YR	$99.1 \pm 1.0$	$0.383^{+0.028}_{-0.033}$	$0.708 \pm 0.019$	-	-	-	$67.38 \pm 0.80$	-
DESI+RSD	$101.7 \pm 2.3$	$0.303^{+0.048}_{-0.071}$	$0.669^{+0.030}_{-0.034}$	$0.215^{+0.11}_{-0.044}$	$0.53 \pm 0.15$	$0.866^{+0.038}_{-0.10}$	$69.13 \pm 1.68$	$0.701^{+0.18}_{-0.096}$
PP+RSD	-	$0.374^{+0.059}_{-0.10}$	$0.714^{+0.068}_{-0.11}$	$0.219^{+0.12}_{-0.069}$	$0.54^{+0.14}_{-0.18}$	$0.878^{+0.038}_{-0.12}$	-	$0.72^{+0.17}_{-0.12}$
DES-5YR+RSD	-	$0.421^{+0.080}_{-0.13}$	$0.738^{+0.088}_{-0.13}$	$0.228^{+0.11}_{-0.070}$	$0.55^{+0.14}_{-0.20}$	$0.874^{+0.044}_{-0.12}$	-	$0.73^{+0.17}_{-0.12}$
DESI+PP+RSD	$100.1 \pm 1.1$	$0.347^{+0.028}_{-0.032}$	$0.692 \pm 0.018$	$0.230^{+0.10}_{-0.034}$	$0.55 \pm 0.15$	$0.864^{+0.042}_{-0.10}$	$68.06 \pm 0.87$	$0.727^{+0.17}_{-0.87}$
DESI+DES-5YR+RSD	$99.0 \pm 1.0$	$0.382^{+0.028}_{-0.032}$	$0.707 \pm 0.018$	$0.232^{+0.11}_{-0.035}$	$0.56 \pm 0.15$	$0.877^{+0.036}_{-0.11}$	$67.38 \pm 0.80$	$0.736^{+0.17}_{-0.088}$

TABLE I. Marginalized  $1\sigma$  C.L. limits of the parameters of the composite model in each of the dataset combinations. Here  $H_0$  (in units of  $\text{km Mpc}^{-1} \text{s}^{-1}$ ) is derived from the inverse-distance-ladder approach utilizing the early-universe prior on  $r_d = 147.09 \pm 0.26 \text{ Mpc}$  [2]. The constraints on  $S_8$  is determined using the relation  $S_8 = \sigma_{8,0} \sqrt{\Omega_{m0}}/0.3$ .

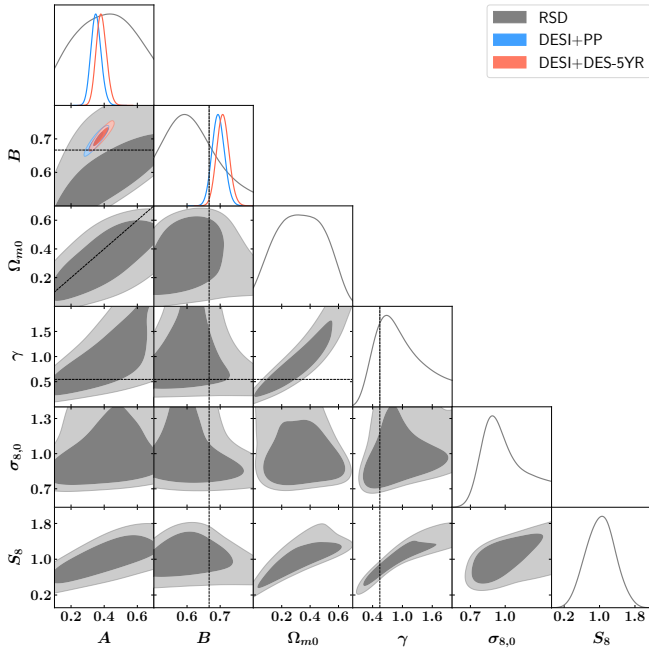


FIG. 3. One-dimensional marginalized posterior distributions, 2-dimensional contour plots at 68% and 95% C.L. limits for parameters of the composite model using RSD data.

post-processing of MCMC chains is done using `GetDist`<sup>2</sup>.

#### IV. RESULTS

The results of our analysis are summarized in Table I, which presents the marginalized constraints on the parameters of the composite model, obtained from different dataset combinations. This table provides an overview of how various observational probes contribute to constraining the parameters governing the background evo-

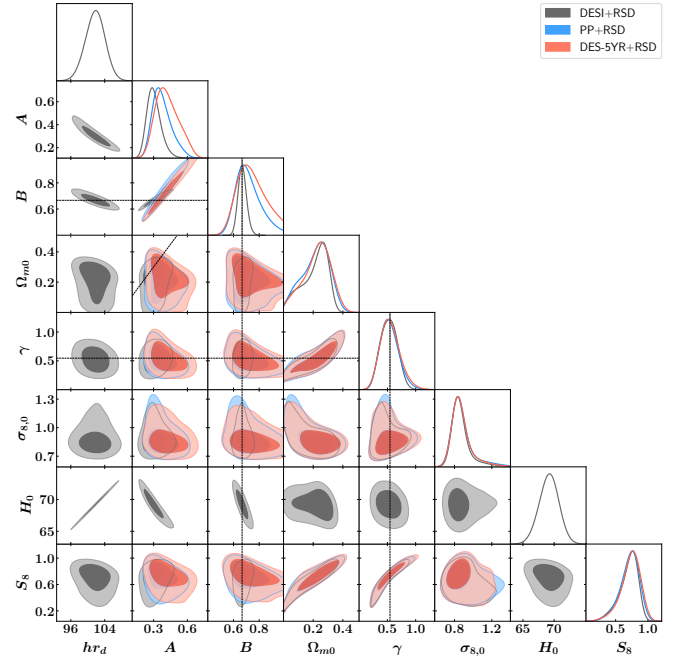


FIG. 4. One-dimensional marginalized posterior distributions, 2-dimensional contour plots at 68% and 95% C.L. limits for parameters of the composite model using RSD in combination with BAO/SNIa data.

lution  $\{hr_d, A, B\}$  and growth rate of cosmic structures  $\{A, B, \Omega_{m0}, \gamma, \sigma_{8,0}\}$  respectively. Our findings can be summarized as follows:

1. When considering only background evolution datasets such as DESI+PP and DESI+DES-5YR, Fig. 2 shows that the parameters  $A$  and  $B$  are well constrained at  $1\sigma$  confidence level (CL). Specifically, for the DESI+PP dataset, we obtain  $A = 0.351^{+0.028}_{-0.032}$  and  $B = 0.694 \pm 0.019$ , while for the DESI+DES-5YR dataset, we find  $A = 0.383^{+0.028}_{-0.033}$  and  $B = 0.708 \pm 0.019$ . In comparison, assuming the Planck  $\Lambda\text{CDM}$  background evolution, we can identify  $A \equiv \Omega_{m0} \approx 0.315$  and  $B \equiv 2/3$ . Thus, our obtained val-

<sup>2</sup> Availalbe at: <https://getdist.readthedocs.io/>

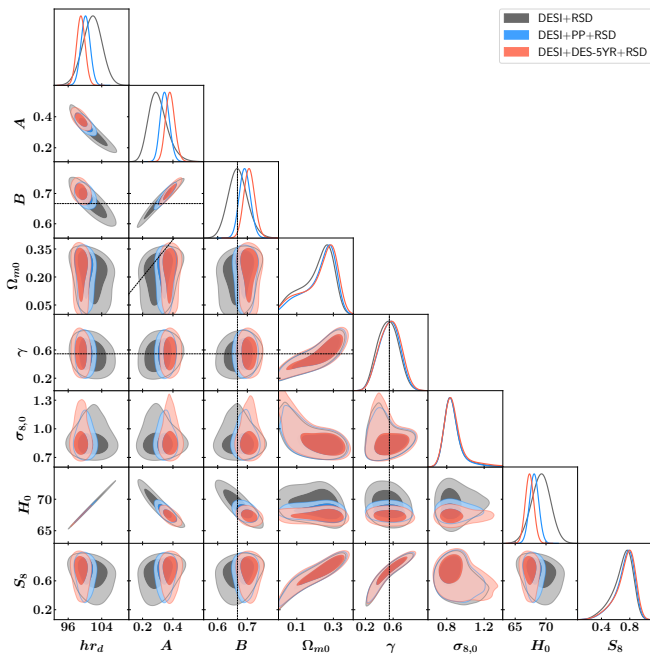


FIG. 5. One-dimensional marginalized posterior distributions, 2-dimensional contour plots at 68% and 95% C.L. limits for parameters of the composite model using combined BAO, SNIa and RSD datasets.

ues indicate deviations from these Planck predictions, with  $A$  differing by  $1.1\sigma$  and  $B$  by  $1.44\sigma$  for DESI+PP, while for DESI+DES-5YR,  $A$  deviates by  $2.02\sigma$  and  $B$  by  $2.2\sigma$  respectively.

- Upon incorporating the RSD data to analyze growth constraints, we find that RSD alone does not impose stringent constraints on the relevant parameters. Fig. 3 shows that both  $B = 2/3$  and  $\gamma = 6/11$  are well within the  $1\sigma$  CL. Additionally, we plot the  $A = \Omega_{m0}$  line which illustrates that, with RSD data alone, the equivalence between  $A$  and  $\Omega_{m0}$  holds within  $1\sigma$  CL. However, the marginalized posteriors for  $A$ ,  $\Omega_{m0}$ ,  $\gamma$ , and  $\sigma_{8,0}$  exhibit non-Gaussian distributions, possibly indicating asymmetries, skewness, or multimodal behaviour in the parameter space. Furthermore, this disparate treatment of the background and perturbation sectors reveals that current RSD measurements are significantly less precise compared to existing BAO and SNIa observations.
- The constraints on the parameters improve when the RSD data is combined with BAO and/or SNIa datasets, as depicted in Fig. 4. The DESI+RSD combination yields  $A = 0.303^{+0.048}_{-0.071}$ ,  $B = 0.669^{+0.030}_{-0.034}$ ,  $\gamma = 0.53 \pm 0.15$ ,  $\Omega_{m0} = 0.215^{+0.11}_{-0.044}$ , and  $\sigma_{8,0} = 0.866^{+0.038}_{-0.10}$ . While the best-fit values of  $A$ ,  $B$  and  $\gamma$  remain close to their  $\Lambda$ CDM counterparts,  $\Omega_{m0}$  exhibits a notable  $1.4\sigma$  deviations from Planck predictions. We also plot the  $A = \Omega_{m0}$  line, revealing that only a small, finite region of the  $A - \Omega_{m0}$  parameter space accommodates

their equivalence within  $1\sigma$ . This suggests a fundamental difference in the behaviour of  $A$  and  $\Omega_{m0}$  at the background and perturbation levels.

- Combining the SNIa (PP or DES-5YR) datasets to RSD further leads to shifts in parameter values. The PP+RSD dataset combination results in deviations for  $A$  ( $1.3\sigma$ ),  $B$  ( $0.55\sigma$ ), and  $\Omega_{m0}$  ( $1.05\sigma$ ) from their respective  $\Lambda$ CDM values, while the best-fit value of  $\gamma$  remains well-consistent with  $\Lambda$ CDM expectations. Similar deviations are observed from  $\Lambda$ CDM when using the DES 5YR+RSD data in place of PP. These findings highlight that BAO and SNIa datasets, when used alongside RSD, significantly improve constraints on the perturbation sector.
- Finally, when combining all three observational probes—BAO, SNIa, and RSD—the constraints become even more refined. The outcomes, presented in Fig. 5, indicate that with DESI+PP+RSD and DESI+DES-5YR+RSD data, the standard  $\Lambda$ CDM value of  $B = 2/3$  falls outside the  $1.4\sigma$  and  $2.2\sigma$  CL, respectively. These results further reinforce the alleged non-equivalence between  $A$  and  $\Omega_{m0}$ , as we find the  $A = \Omega_{m0}$  line is just marginally allowed at  $1\sigma$  with the DESI+PP+RSD data, and at  $2\sigma$  with the DESI+DES-5YR+RSD data. Nevertheless, the best-fit values of  $\gamma$ , in both cases, remain in excellent agreement with the theoretical expectation of  $\gamma = 6/11$ .
- The low redshifts observational data that we use in this analysis do not directly constrain the  $H_0$  parameter but the combination  $hr_d$  through the BAO measurements. We use the Planck-2018 prior on  $r_d$  assuming that there is no new physics in the early Universe and obtain the constraint on  $H_0$  from different data combinations, which is shown in Table I. For the DESI+RSD combination, we find a constrained value of  $H_0 = 69.13 \pm 1.68$  km Mpc $^{-1}$  s $^{-1}$ , which naturally accommodates  $H_0$  from Planck ( $67.4 \pm 0.5$  km Mpc $^{-1}$  s $^{-1}$ ) and  $H_0$  from SH0ES ( $73.04 \pm 1.04$  km Mpc $^{-1}$  s $^{-1}$ ) at approximately  $2\sigma$ . When SNIa datasets are included, the constraints become more precise as shown in Fig 5.
- For the  $\sigma_{8,0}$  parameter, we observe that the marginalized posteriors are non-Gaussian with extended tails to the right. However, the mean values are consistent with the Planck 2018 best-fit values within  $1\sigma$ . On the other hand, the  $S_8$  parameter shows constrained mean values that are closer to those obtained from weak lensing measurements, mainly due to a reduced mean value of  $\Omega_{m0}$ . This reduction is achieved by separating the background and perturbation sectors, introducing a non-equivalence between  $A$  (in the background universe) and  $\Omega_{m0}$  (in the growth of structures). As a result, while  $\sigma_{8,0}$  (a derived parameter in CMB analysis) remains consistent with Planck CMB values, the final constraints on  $S_8$  align well with the

best-fit values from large-scale structure, galaxy clustering, and lensing surveys, where  $S_8$  is directly sampled as a cosmological parameter. Therefore, our composite framework demonstrates the ability to simultaneously address the  $\sigma_8$  and  $S_8$  tensions through the non-equivalence between  $A$  and  $\Omega_{m0}$ .

8. The existing RSD data alone do not provide precise constraints on all parameters (see Fig. 3) when compared to the background datasets from DESI+PP and DESI+DES-5YR. However, the inclusion of DESI leads to more precise constraints on parameters like  $hr_d$ ,  $A$ , and  $B$ , with these constraints becoming even tighter when DESI is combined with PP and DES-5YR data (see Fig. 5). Once  $A$  and  $B$  are well-constrained, the RSD data then refines the remaining parameters,  $\Omega_{m0}$ ,  $\sigma_{8,0}$ , and  $\gamma$ , within the parameter space defined by the prior constraints on  $A$  and  $B$ , which are consistent with the background datasets. Given their current level of precision, the existing RSD data do not play a significant role in determining background evolution when combined with DESI and SNIa data. Interestingly, when only DESI data are considered, the values of  $A$  and  $B$  align closely with the best-fit  $\Lambda$ CDM values ( $A = 0.315$ ,  $B = 2/3$ ). Yet, the addition of SNIa data results in noticeable shifts in the mean values of  $A$  and  $B$ , with these shifts being more pronounced with DES-5YR compared to that of PP. This suggests the possibility of presence of new physics or unidentified systematics in the SNIa data.
9. As we mention in the beginning, the background expansion is mainly controlled by two parameters:  $A$  and  $B$  while the perturbed Universe is controlled by  $\gamma$ ,  $\Omega_{m0}$  and  $\sigma_{8,0}$ . A  $\Lambda$ CDM Universe, both at background level as well as at perturbed level, demands  $B = 2/3$ ,  $\gamma = 6/11$  and  $A = \Omega_{m0}$ . All these conditions should be simultaneously satisfied for  $\Lambda$ CDM Universe. Violations of any of these conditions shows breakdown of  $\Lambda$ CDM model. Our results, as depicted in Fig 5, show that, at present, there is not much correlation between the background parameters and perturbation parameters. This is mainly due to less constraining  $f\sigma_8$  data. But with more precise data for the growth history of the Universe, as expected from upcoming Stage-IV missions like Euclid [53, 54], we expect a larger correlation between background and perturbation parameters and stronger signatures for new physics both at the background and perturbed levels of the Universe. We study such expected signals in the next section.

## V. FORECAST

As discussed in the previous section, the current RSD data do not significantly constrain the background parameters when combined with BAO and SNIa observations. Instead, the constraints on these parameters

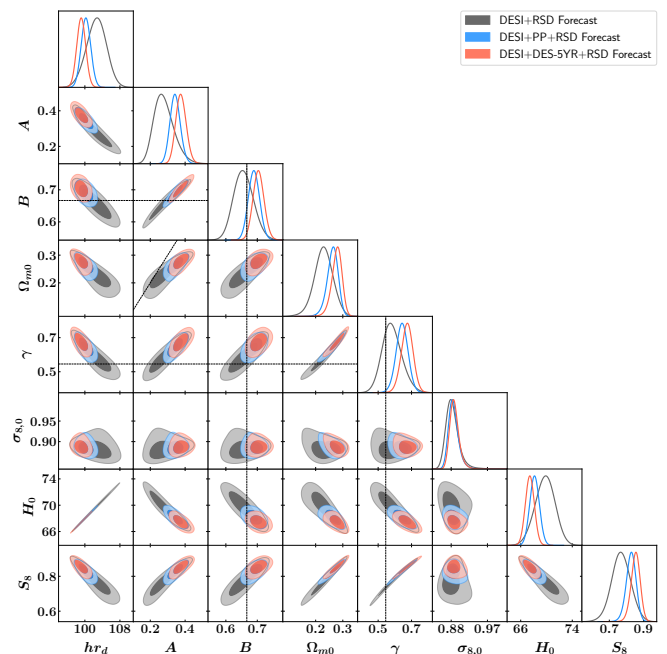


FIG. 6. Forecast on one-dimensional marginalized posterior distributions, 2-dimensional contour plots at 68% and 95% C.L. limits for parameters of the composite model using combined BAO, SNIa and modified RSD datasets.

are entirely determined by the BAO and SNIa datasets. Given this, the role of RSD data is to constrain the parameters governing the growth of perturbations within the background parameter space already constrained by BAO and SNIa. However, the resulting constraints have large confidence intervals and exhibit no correlation with the background parameters.

To examine the potential impact of improved RSD precision, we modify the existing RSD data by reducing the error bars by 10% at each data point while keeping the central values unchanged. This level of improvement is expected from future Stage-IV surveys such as Euclid [55, 56]. The resulting constraints and posterior distributions will provide insights into how enhanced RSD precision can refine our understanding of the underlying cosmology.

The results of this analysis are summarized in Fig. 6 and Table II. We observe that the parameters in the perturbation sector are now more tightly constrained, with significantly reduced error bars. Additionally, a clear positive correlation between  $A$ ,  $B$  and  $\gamma$ ,  $\Omega_{m0}$  emerges. In the analysis with the current RSD data, this correlation is largely suppressed (see Fig. 5) due to the limited precision of the existing RSD measurements. Thus, RSD data with improved precision is expected to influence not only the constraints on the perturbation sector but also those on the background parameters.

Notably, we find that  $\gamma = 6/11$  and  $A = \Omega_{m0}$  line fall outside the  $2\sigma$  confidence intervals in the DESI+PP+RSD and DESI+DES-5YR+RSD combina-

Datasets	$hr_d$	$A$	$B$	$\Omega_{m0}$	$\gamma$	$\sigma_{s,0}$	$H_0$	$S_8$
DESI+RSD Forecast	$102.6 \pm 2.2$	$0.279_{-0.064}^{+0.046}$	$0.657_{-0.033}^{+0.029}$	$0.229 \pm 0.034$	$0.583_{-0.063}^{+0.052}$	$0.883_{-0.018}^{+0.011}$	$69.8 \pm 1.5$	$0.769 \pm 0.056$
DESI+PP+RSD Forecast	$100.2 \pm 1.1$	$0.343 \pm 0.029$	$0.690 \pm 0.018$	$0.262_{-0.017}^{+0.022}$	$0.643 \pm 0.036$	$0.8860_{-0.014}^{+0.0093}$	$68.15 \pm 0.73$	$0.827_{-0.026}^{+0.030}$
DESI+DES-5YR+RSD Forecast	$99.2 \pm 1.0$	$0.377 \pm 0.030$	$0.704 \pm 0.018$	$0.278_{-0.016}^{+0.021}$	$0.674 \pm 0.035$	$0.8882_{-0.013}^{+0.0090}$	$67.42 \pm 0.69$	$0.854_{-0.025}^{+0.028}$

TABLE II. Forecast on marginalized  $1\sigma$  C.L. limits of the composite model parameters from different dataset combinations with modified RSD dataset. Here  $H_0$  (in units of  $\text{km Mpc}^{-1} \text{s}^{-1}$ ) is derived from the inverse-distance-ladder approach utilizing the early-universe prior on  $r_d = 147.09 \pm 0.26 \text{ Mpc}$  [2]. The constraints on  $S_8$  are determined using the relation  $S_8 = \sigma_{s,0} \sqrt{\Omega_{m0}/0.3}$ .

tions. Furthermore, the intersection point of  $B = 2/3$  and  $\gamma = 6/11$  is excluded at the  $2\sigma$  level in DESI+DES-5YR+RSD, while it is marginally included in the  $2\sigma$  confidence interval in DESI+PP+RSD. However, it is important to emphasize that in this study, we have kept the central values of  $f\sigma_8$  fixed while only reducing the error bars. In contrast, future observational data may yield different central values. Therefore, this forecast should not be interpreted as providing definitive conclusions about the underlying cosmology. Instead, it serves as a guiding framework to assess the potential impact of future RSD data with enhanced precision in constraining both the physics of background evolution and the growth of perturbations.

## VI. CONCLUSIONS

For a comprehensive understanding of the underlying cosmology, it is essential to disentangle and independently constrain the growth of perturbations from the background dynamics. In this work, we have investigated potential signatures of new physics by analyzing deviations from the  $\Lambda\text{CDM}$  model in both the background evolution and the growth of perturbations. To achieve this, we have introduced separate parameterizations for deviations in these two sectors, allowing us to systematically assess any new imprints beyond the standard  $\Lambda\text{CDM}$  framework.

In the background sector, we implemented deviations by modifying the late-time evolution of the scale factor. This approach is particularly robust, as it can encapsulate effects arising from both modified DE and MG. The deviations are described by two parameters,  $A$  and  $B$ , which reduce to  $\Omega_{m0}$  and  $2/3$ , respectively, in the standard  $\Lambda\text{CDM}$  scenario. To probe deviations in the growth of structures, we introduced a new fitting function for  $f\sigma_8$ , which parameterizes possible departures from  $\Lambda\text{CDM}$  through the growth index  $\gamma$ . In the standard  $\Lambda\text{CDM}$  model,  $\gamma$  is known to take the value  $6/11$ . We have constrained the background and perturbation parameters using SN-Ia and BAO data, as well as growth rate measurements from RSD.

We find that the background parameters,  $A$  and  $B$ , are primarily constrained by SN-Ia and BAO observations, while RSD data predominantly constrain the parameters associated with the perturbation sector, namely  $\Omega_{m0}$ ,  $\gamma$ ,

and  $\sigma_{s,0}$ , with minimal impact on  $A$  and  $B$ . Our analysis provides significant evidence for deviations from the  $\Lambda\text{CDM}$  model in both background evolution and structure growth. Specifically, using the DESI+PP+RSD and DESI+DES-5YR+RSD combinations, we find that  $B = 2/3$  is excluded at  $1.4\sigma$  and  $2.2\sigma$  CL, respectively, while the  $A = \Omega_{m0}$  line remains marginally allowed at  $1\sigma$  in the former case and at  $2\sigma$  in the latter.

Interestingly, the best-fit value of  $\gamma$  in our analysis is close to the  $\Lambda\text{CDM}$  expectation, in contrast to previous studies that assumed a fixed  $\Lambda\text{CDM}$  background. For instance, the authors of [40] obtained  $\gamma = 0.639_{-0.025}^{+0.024}$ , excluding  $\gamma = 6/11$  at a statistical significance of  $4.2\sigma$ . In our case, the inclusion of modifications in the background evolution through the parameters  $A$  and  $B$  leads to a best-fit value of  $\gamma$  that is closer to  $6/11$ . This difference can be attributed to a lower mean value of  $\Omega_{m0}$ , which we have found in our analysis. This trend is also expected from the positive correlation between  $\Omega_{m0}$  and  $\gamma$ , as illustrated in Fig. 5.

Therefore, our results indicate that while the growth of structures is consistent with the predictions of GR, the data favour a lower value of  $\Omega_{m0}$  compared to  $\Lambda\text{CDM}$ . This, in turn, suggests that observational data exhibit a stronger preference for modifications in the background evolution, likely due to an evolving DE component, rather than modifications to gravity itself.

Motivated by our findings with the current RSD data that it does not significantly constrain the background parameters when combined with SN-Ia and BAO datasets, and no apparent correlation is observed between the parameters governing the background and perturbations—we investigated the potential impact of more precise RSD data from future surveys on constraining the underlying cosmology. Our analysis suggests that even a 10% improvement in precision could play a crucial role in detecting possible new physics in both the perturbation and background sectors. This is because a correlation between the background and perturbation parameters is expected to emerge, which is currently suppressed due to the limited precision of existing RSD data.

In conclusion, the non-equivalence of  $A$  and  $\Omega_{m0}$  could serve as a key indicator of new physics in the background sector. This suggests that a modification of DE should account for this discrepancy. We are currently exploring models with an evolving DE component to further investigate this possibility.

## ACKNOWLEDGMENTS

SGC acknowledges funding from the Anusandhan National Research Foundation (ANRF), Govt. of India, under the National Post-Doctoral Fellowship (File no.

PDF/2023/002066). PM acknowledges funding from ANRF, Govt. of India, under the National Post-Doctoral Fellowship (File no. PDF/2023/001986). AAS acknowledges the funding from ANRF, Govt. of India, under the research grant no. CRG/2023/003984. We acknowledge the use of the HPC facility, Pegasus, at IUCAA, Pune, India.

- 
- [1] P. J. E. Peebles (2024) [arXiv:2405.18307 \[astro-ph.CO\]](#).
- [2] N. Aghanim *et al.* (Planck), *Astron. Astrophys.* **641**, A6 (2020), [Erratum: *Astron. Astrophys.* 652, C4 (2021)], [arXiv:1807.06209 \[astro-ph.CO\]](#).
- [3] P. A. R. Ade *et al.* (Planck), *Astron. Astrophys.* **594**, A14 (2016), [arXiv:1502.01590 \[astro-ph.CO\]](#).
- [4] S. Aiola *et al.* (ACT), *JCAP* **12**, 047 (2020), [arXiv:2007.07288 \[astro-ph.CO\]](#).
- [5] E. Aubourg *et al.* (BOSS), *Phys. Rev. D* **92**, 123516 (2015), [arXiv:1411.1074 \[astro-ph.CO\]](#).
- [6] S. Alam *et al.* (BOSS), *Mon. Not. Roy. Astron. Soc.* **470**, 2617 (2017), [arXiv:1607.03155 \[astro-ph.CO\]](#).
- [7] G. E. Addison, D. J. Watts, C. L. Bennett, M. Halpern, G. Hinshaw, and J. L. Weiland, *Astrophys. J.* **853**, 119 (2018), [arXiv:1707.06547 \[astro-ph.CO\]](#).
- [8] B. S. Haridasu, V. V. Luković, and N. Vittorio, *JCAP* **05**, 033 (2018), [arXiv:1711.03929 \[astro-ph.CO\]](#).
- [9] A. G. Riess, *Nature Rev. Phys.* **2**, 10 (2019), [arXiv:2001.03624 \[astro-ph.CO\]](#).
- [10] D. M. Scolnic *et al.* (Pan-STARRS1), *Astrophys. J.* **859**, 101 (2018), [arXiv:1710.00845 \[astro-ph.CO\]](#).
- [11] A. G. Adame *et al.* (DESI), (2024), [arXiv:2404.03002 \[astro-ph.CO\]](#).
- [12] D. Rubin *et al.*, (2023), [arXiv:2311.12098 \[astro-ph.CO\]](#).
- [13] T. M. C. Abbott *et al.* (DES), *Astrophys. J. Lett.* **973**, L14 (2024), [arXiv:2401.02929 \[astro-ph.CO\]](#).
- [14] D. Brout *et al.*, *Astrophys. J.* **938**, 110 (2022), [arXiv:2202.04077 \[astro-ph.CO\]](#).
- [15] A. G. Riess *et al.*, *Astrophys. J. Lett.* **934**, L7 (2022), [arXiv:2112.04510 \[astro-ph.CO\]](#).
- [16] E. Di Valentino *et al.*, *Astropart. Phys.* **131**, 102604 (2021), [arXiv:2008.11285 \[astro-ph.CO\]](#).
- [17] S. Weinberg, in *4th International Symposium on Sources and Detection of Dark Matter in the Universe (DM 2000)* (2000) pp. 18–26, [arXiv:astro-ph/0005265](#).
- [18] E. Di Valentino, O. Mena, S. Pan, L. Visinelli, W. Yang, A. Melchiorri, D. F. Mota, A. G. Riess, and J. Silk, *Class. Quant. Grav.* **38**, 153001 (2021), [arXiv:2103.01183 \[astro-ph.CO\]](#).
- [19] E. Abdalla *et al.*, *JHEAp* **34**, 49 (2022), [arXiv:2203.06142 \[astro-ph.CO\]](#).
- [20] M. Chevallier and D. Polarski, *Int. J. Mod. Phys. D* **10**, 213 (2001), [arXiv:gr-qc/0009008](#).
- [21] E. V. Linder, *Phys. Rev. Lett.* **90**, 091301 (2003), [arXiv:astro-ph/0208512](#).
- [22] E. V. Linder, *Phys. Rev. D* **72**, 043529 (2005), [arXiv:astro-ph/0507263](#).
- [23] S. Capozziello, V. F. Cardone, E. Piedipalumbo, and C. Rubano, *Class. Quant. Grav.* **23**, 1205 (2006), [arXiv:astro-ph/0507438](#).
- [24] T. P. Sotiriou and V. Faraoni, *Rev. Mod. Phys.* **82**, 451 (2010), [arXiv:0805.1726 \[gr-qc\]](#).
- [25] S. Nojiri, S. D. Odintsov, and V. K. Oikonomou, *Phys. Rept.* **692**, 1 (2017), [arXiv:1705.11098 \[gr-qc\]](#).
- [26] Y. Fujii and K. ichi Maeda, *Classical and Quantum Gravity* **20**, 4503 (2003).
- [27] K. Freese and M. Lewis, *Phys. Lett. B* **540**, 1 (2002), [arXiv:astro-ph/0201229](#).
- [28] G. R. Dvali, G. Gabadadze, and M. Porrati, *Phys. Lett. B* **485**, 208 (2000), [arXiv:hep-th/0005016](#).
- [29] T. Barreiro and A. A. Sen, *Phys. Rev. D* **70**, 124013 (2004), [arXiv:astro-ph/0408185](#).
- [30] V. Sahni and A. Starobinsky, *Int. J. Mod. Phys. D* **15**, 2105 (2006), [arXiv:astro-ph/0610026](#).
- [31] T. Holsclaw, U. Alam, B. Sanso, H. Lee, K. Heitmann, S. Habib, and D. Higdon, *Phys. Rev. Lett.* **105**, 241302 (2010), [arXiv:1011.3079 \[astro-ph.CO\]](#).
- [32] T. Holsclaw, U. Alam, B. Sanso, H. Lee, K. Heitmann, S. Habib, and D. Higdon, *Phys. Rev. D* **84**, 083501 (2011), [arXiv:1104.2041 \[astro-ph.CO\]](#).
- [33] M. Sahlén, A. R. Liddle, and D. Parkinson, *Phys. Rev. D* **72**, 083511 (2005).
- [34] D. Huterer and G. Starkman, *Phys. Rev. Lett.* **90**, 031301 (2003).
- [35] A. A. Starobinsky, *JETP Lett.* **68**, 757 (1998), [arXiv:astro-ph/9810431](#).
- [36] D. Huterer and M. S. Turner, *Phys. Rev. D* **60**, 081301 (1999), [arXiv:astro-ph/9808133](#).
- [37] A. A. Sen and S. Sethi, *Phys. Lett. B* **532**, 159 (2002), [arXiv:gr-qc/0111082](#).
- [38] A. A. Sen, *JCAP* **03**, 010 (2006), [arXiv:astro-ph/0512406](#).
- [39] D. Huterer, *Astron. Astrophys. Rev.* **31**, 2 (2023), [arXiv:2212.05003 \[astro-ph.CO\]](#).
- [40] N.-M. Nguyen, D. Huterer, and Y. Wen, *Phys. Rev. Lett.* **131**, 111001 (2023), [arXiv:2302.01331 \[astro-ph.CO\]](#).
- [41] U. Mukhopadhyay, S. Haridasu, A. A. Sen, and S. Dhawan, *Phys. Rev. D* **110**, 123516 (2024), [arXiv:2407.10845 \[astro-ph.CO\]](#).
- [42] J. N. Fry, *Phys. Lett. B* **158**, 211 (1985).
- [43] L.-M. Wang and P. J. Steinhardt, *Astrophys. J.* **508**, 483 (1998), [arXiv:astro-ph/9804015](#).
- [44] E. V. Linder and R. N. Cahn, *Astropart. Phys.* **28**, 481 (2007), [arXiv:astro-ph/0701317](#).
- [45] Y. Gong, *Phys. Rev. D* **78**, 123010 (2008), [arXiv:0808.1316 \[astro-ph\]](#).
- [46] B. O. Sánchez *et al.* (DES), *Astrophys. J.* **975**, 5 (2024), [arXiv:2406.05046 \[astro-ph.CO\]](#).
- [47] S. Nesseris, G. Pantazis, and L. Perivolaropoulos, *Phys. Rev. D* **96**, 023542 (2017), [arXiv:1703.10538 \[astro-ph.CO\]](#).
- [48] B. Sagredo, S. Nesseris, and D. Sapone, *Phys. Rev. D* **98**, 083543 (2018), [arXiv:1806.10822 \[astro-ph.CO\]](#).

- [49] F. Skara and L. Perivolaropoulos, *Phys. Rev. D* **101**, 063521 (2020), arXiv:1911.10609 [astro-ph.CO].
- [50] C. Blake *et al.*, *Mon. Not. Roy. Astron. Soc.* **425**, 405 (2012), arXiv:1204.3674 [astro-ph.CO].
- [51] G.-B. Zhao *et al.* (eBOSS), *Mon. Not. Roy. Astron. Soc.* **482**, 3497 (2019), arXiv:1801.03043 [astro-ph.CO].
- [52] E. Macaulay, I. K. Wehus, and H. K. Eriksen, *Phys. Rev. Lett.* **111**, 161301 (2013), arXiv:1303.6583 [astro-ph.CO].
- [53] L. Amendola *et al.*, *Living Rev. Rel.* **21**, 2 (2018), arXiv:1606.00180 [astro-ph.CO].
- [54] Y. Mellier *et al.* (Euclid), (2024), arXiv:2405.13491 [astro-ph.CO].
- [55] A. Blanchard *et al.* (Euclid), *Astron. Astrophys.* **642**, A191 (2020), arXiv:1910.09273 [astro-ph.CO].
- [56] N. Hamaus *et al.* (Euclid), *Astron. Astrophys.* **658**, A20 (2022), arXiv:2108.10347 [astro-ph.CO].